

Differential Cross Sections Measurement for the $pp \rightarrow d\pi^+$ Reaction at 850 MeV/c

M. Betigeri ⁱ, J. Bojowald ^a, A. Budzanowski ^d, A. Chatterjee ⁱ, J. Ernst ^g, L. Freindl ^d,
D. Frekers ^h, W. Garske ^h, K. Grewer ^h, A. Hamacher ^a, J. Ilieva ^{a,e}, L. Jarczyk ^c,
K. Kilian ^a, S. Kliczewski ^d, W. Klimala ^{a,c}, D. Kolev ^f, T. Kutsarova ^e, J. Lieb ^j,
H. Machner ^a, A. Magiera ^c, H. Nann ^a, L. Pentchev ^e, D. Protić ^a, B. Razen ^a,
P. von Rossen ^a, B. J. Roy ⁱ, R. Siudak ^d, A. Strzałkowski ^c, R. Tsenov ^f, K. Zwoll ^b

a. Institut für Kernphysik, Forschungszentrum Jülich, Jülich, Germany

b. Zentrallabor für Elektronik, Forschungszentrum Jülich, Jülich, Germany

c. Institute of Physics, Jagellonian University, Krakow, Poland

d. Institute of Nuclear Physics, Krakow, Poland

e. Institute of Nuclear Physics and Nuclear Energy, Sofia, Bulgaria

f. Physics Faculty, University of Sofia, Sofia, Bulgaria

g. Institut für Strahlen- und Kernphysik der Universität Bonn, Bonn, Germany

h. Institut für Kernphysik, Universität Münster, Münster, Germany

i. Nuclear Physics Division, BARC, Bombay, India

j. Physics Department, George Mason University, Fairfax, Virginia, USA

(Dated: November 6, 2018)

A stack of annular detectors made of high purity germanium and a magnet spectrograph were used to measure $pp \rightarrow d\pi^+$ differential cross sections at a beam momentum of 850 MeV/c over a large angular range. A total cross section of $\sigma = 0.2301 \pm 0.0036$ (*stat*) ± 0.0230 (*syst*) mb and an anisotropy $A_2/A_0 = 0.856 \pm 0.016$ were deduced. These values follow fits to low energy data. From the present A_2 value it is found that the pionic p-wave amplitude a_0 is larger than assumed so far.

PACS numbers:

I. INTRODUCTION

Although the reaction $pp \rightarrow d\pi^+$ has been intensively studied, some open problems remain. These are mainly connected to the importance of different partial wave amplitudes. For small pion energies only three complex amplitudes are believed to contribute to the physical observables: a_0 , a_1 and a_2 . Here the index denotes the angular momentum in the proton–proton channel. Close to threshold, the cross section is given by only one amplitude a_1 corresponding to an s-wave in the final channel. For slightly larger energies, the p-wave amplitudes a_0 and a_2 show up. Because $|a_2|$ is much larger than $|a_0|$, the latter amplitude is often ignored [1]. The d-wave amplitudes are even smaller. In the simplest experiments, three observables can be measured, the total cross section, the anisotropy and the asymmetry of the reaction products. The usual method to deduce the three complex amplitudes is then to make use of the Watson theorem [2]. However, this procedure often yields negative values for $|a_0|$ [3]. Because of its smallness, the magnitude of a_0 cannot be extracted from the total cross section. It enters the other two quantities via interference with other amplitudes. Especially in the anisotropy, there is an interference between the two p-waves. Thus the measurement of this quantity might yield an estimate of a_0 .

The energy dependence of the anisotropy, which will be defined later, is a puzzle. Data published before 1996 like those of Ref. [4] lie on but of-

ten below the predictions of the SP96 phase shift analysis carried out by the Virginia group [5]. Near threshold data, appeared first in 1996 [6, 7] and are in agreement with the SP96 solution. The newest data are from a measurement of the inverse reaction [8]. They are even below the Ritchie et al. data [4], thus indicating the negligible effect of a_0 even in the interference term (see section III). This is in contrast to SAID calculations as well as to extrapolation of the new near threshold results. Furthermore, the new data of Ref. [8] show a much larger scattering than the threshold data, although the latter are from two different experiments. It is worth mentioning that in the measurement of the anisotropy, the luminosity cancels out. Large fluctuations in this quantity may thus point to systematic errors other than target thickness and beam intensity. We, therefore, investigate the situation by a measurement in the range of these data not so close to threshold.

In the present experiment, the differential cross section for the $pp \rightarrow d\pi^+$ reaction was measured at a beam momentum of 850 MeV/c, which corresponds to a pion centre of mass momentum divided by the pion rest mass of $\eta = 0.51$. This value is within the range of the Pasyuk et al. data [8] and will thus allow to proof the importance of pp -wave interference in the anisotropy as already mentioned.

II. EXPERIMENTAL PROCEDURE

The measurement of the reaction $pp \rightarrow d\pi^+$ was performed using a detector that combines large momentum and geometrical acceptance for heavy recoiling reaction products. A proton beam with a momentum of 850 MeV/c was extracted from the COSY accelerator and focused onto a target cell containing liquid hydrogen. It had a diameter of 6 mm and a thickness of 6.4 ± 0.3 mm [10] with windows of 1.5 μm Mylar. The excellent ratio of hydrogen to heavier nuclei in the window material reduced empty target events to a negligible level. The beam spot had dimensions of less than 1 mm and divergences of better than 4 mrad. Beam halo events were suppressed using a plastic scintillator as a veto counter with a 4mm diameter inner hole in front of the target. The detector system is the “Germanium Wall”, which is part of the GEM-detector at COSY in Jülich [11] and the remodelled magnetic spectrograph Big Karl [6]. Here we give only some additional details specific for this experiment.

The magnetic spectrograph was set to zero degrees in the laboratory system. It was used to measure the low energy branch of deuterons close to the primary beam. The germanium wall consists of three high purity germanium detectors with radial symmetry with respect to the beam axis. The first detector (called Quirl-detector) measures the position and the energy loss of the penetrating particles. The active area of the diode is divided on both sides into 200 segments by 200 grooves. Each groove is shaped as an Archimedes’ spiral covering an angular range of 2π . They are mainly used for measuring the energy loss of the penetrating particles or the total kinetic energy of stopped particles, respectively. The next detectors are divided into 32 wedges to reduce the counting rate per division leading to a higher maximum total counting rate of the whole detector.

Fig. 1 shows the response of the germanium wall for reaction particles. Clearly distinguished are two bands corresponding to protons from the $pp \rightarrow pp\pi^0$ and deuterons from the $pp \rightarrow d\pi^+$ reactions. The quantities measured with the germanium wall are energy, emission vertex and particle type. They were converted to a four-momentum vector. These measurements and the knowledge of the four momenta in the initial state yield the missing mass of the unobserved pion by applying conservation of momentum, energy, charge and baryon number.

The germanium detectors have holes in their centres. The primary beam passes through these holes and is then led via an exit in a side yoke of the first dipole magnet of the magnetic spectrograph to a well shielded beam dump. Recoiling deuterons at emission angles inside this hole, i. e. close to

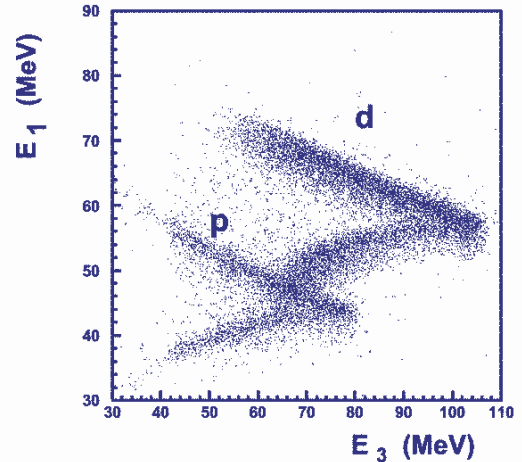


FIG. 1: Energy loss in the first calorimeter crystal E_1 versus the loss in the second named E_3 (A possible crystal E_2 was not mounted in this experiment). The visible bands are due to detected protons and deuterons.

zero degree, were detected by the magnetic spectrograph. Details of such measurements are given in Ref. [6].

The reaction deuterons were selected in the offline analysis by applying gates to the kinematical loci in Fig. 1. The efficiency of the analysis procedures were studied by Monte Carlo calculations [12]. Finally, the data were corrected for reduced efficiencies due to nuclear absorption in the detector material [13]. The correction factors vary from 17% to 22% for the present energy interval. The present setup has full acceptance for the recoiling deuterons, except for a small area close to the beam exit hole. For particles not stopped in the germanium wall, only energy loss measurements are made. Because the angular distribution of the reaction products must be symmetric to 90 degree in the centre of mass system, it is sufficient to measure only one half of the distribution. The deuterons emitted backward in the centre of mass system are all stopped in the germanium wall. We restrict ourselves to this part of the distribution in

order to not introduce ambiguities when unfolding the backbending part in Fig. 1.

Each of the measurements, i. e. emission angle $\Omega = (\theta, \phi)$ and energy of the recoiling deuteron, is sufficient to extract the angular distribution. Because of this overconstraint, one can clearly distinguish between reaction and background events. This is shown in Fig. 2. The missing mass of

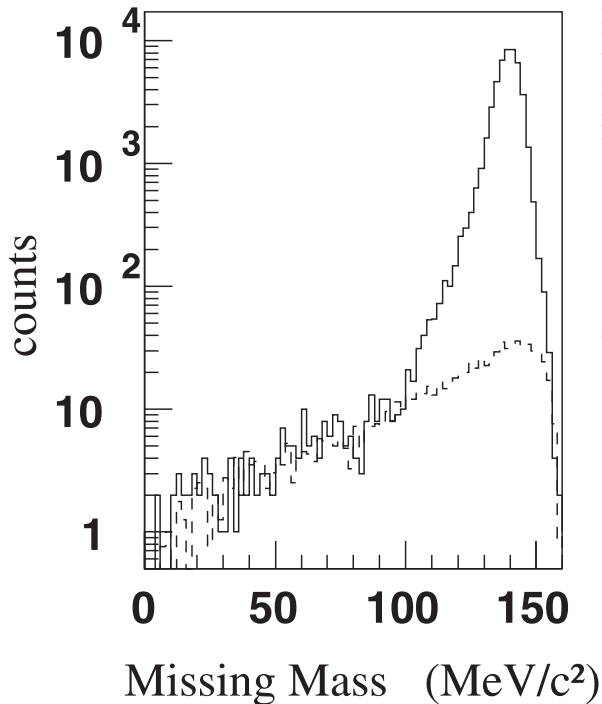


FIG. 2: Missing mass spectrum. The experimental result is shown by solid line histogram, the assumed background by dashed line histogram.

the unobserved π^+ is shown as deduced in the off line analysis. The distribution has a resolution of $5.9 \text{ MeV}/c^2$. The logarithmic scale was chosen to make the small background visible. The background, shown by a dashed curve in Figure 2, was measured with an empty target, normalized to integrated beam intensity and then subtracted.

Finally, the counts were converted to cross sections by normalizing to the target thickness and number of beam protons. The latter were measured with calibrated luminosity monitor counters. In the calibration procedure the direct beam intensity and the corresponding number of scattered

particles are compared. The former was measured³ with the trigger hodoscope in the focal plane of the magnet spectrograph. This number is of course much larger and lead to dead time in the hodoscope. The beam intensity was then reduced by debunching the beam between the ion source and the cyclotron injector. For sufficiently small beam intensity the relation between monitors and hodoscope is linear. The counting rate in the monitors was in the the production runs small enough to have dead time effects on a negligible level. This procedure yields a systematic uncertainty of 5% for the beam intensity. This yields together with the target thickness uncertainty of also 5% a maximal total systematical error of 10% for the overall normalization of the differential cross section when both errors are added linearly.

III. RESULTS

The measured angular distribution in the centre of mass system are shown in Fig. 3. The point

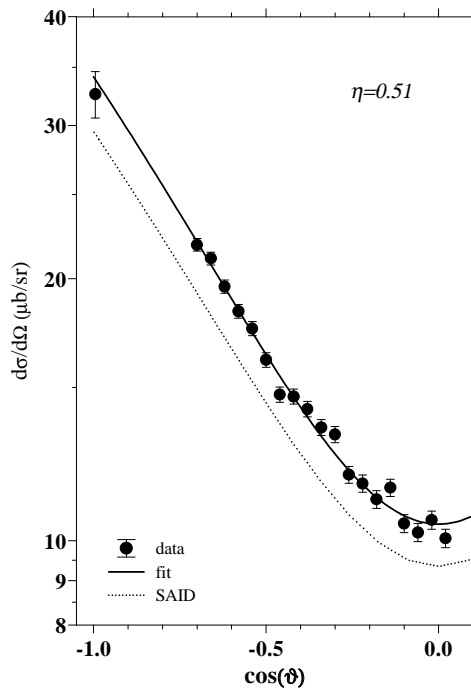


FIG. 3: The measured angular distribution is shown by the full symbols. Shown are the statistical errors only. The overall normalization of the cross section has total systematical error of 10%. The solid curve is a Legendre polynomial fit up to second order, the dotted curve the SP96 solution [5].

near $\cos(\theta) = -1$ was measured with the magnetic spectrograph. It has larger statistical error than

all other points which were measured with the germanium wall. This is due to its small acceptance. The data show a very strong anisotropy when compared to those close to the threshold [6, 7]. This is an indication of the p-wave strength and thus of the importance of the intermediate Δ -p system. The angular distribution was fitted by a series of Legendre polynomials $P_{2L}[\cos(\theta)]$

$$4\pi \frac{d\sigma(\theta)}{d\Omega} = A_0 + A_2 P_2[\cos(\theta)] + A_4 P_4[\cos(\theta)]. \quad (1)$$

The fitted parameters A_{2L} are connected with amplitudes a_i

$$A_0 = \sigma = \frac{1}{4}[|a_0|^2 + |a_1|^2 + |a_2|^2 + C(|d|^2)] \quad (2)$$

where $C(|d|^2)$ represents all d-wave contributions,

$$\begin{aligned} A_2 = & \frac{1}{4}|a_2|^2 + \frac{3}{14}|a_6|^2 - \sqrt{1/2}\Re(a_0 a_2^*) \\ & + \sqrt{1/8}\Re(a_1 a_3^*) + \sqrt{5/8}\Re(a_1 a_4^*) \\ & + \frac{1}{2}\sqrt{5/7}\Re(a_1 a_5^*) + \sqrt{1/2}\Re(a_1 a_6^*) \\ & + D(|d|^2) + E(dd) \end{aligned} \quad (3)$$

with $D(|d|^2)$ denoting other d-wave contributions and $E(dd)$ terms with interferences between two d-waves. A_4 is given by

$$\begin{aligned} A_4 = & -\frac{5}{49}|a_5|^2 + \frac{1}{28}|a_6|^2 + \frac{9}{14}\Re(a_3 a_6^*) \\ & + \frac{10}{49}\sqrt{14}\Re(a_4 a_5^*) + \frac{5}{14}\sqrt{5}\Re(a_4 a_6^*) \\ & + \frac{5}{7}\sqrt{\frac{5}{14}}\Re(a_5 a_6^*). \end{aligned} \quad (4)$$

The amplitude a_1 is the s-wave in the pion-deuteron channel, a_0 and a_2 denote p-waves and a_3 to a_6 denote d-waves. In Eqs. 2 to 4 the notation of Mandl and Regge [9] is used. The total cross section can near threshold be written as

$$\sigma = \alpha_0 \eta + \alpha_1 \eta^3. \quad (5)$$

The first term corresponds to the s-wave amplitude a_1 and the second to the two p-wave amplitudes a_0 and a_2 .

Fits of Eq. 1 up to second and to fourth order were performed. Although the χ^2 -values of both fits are similar, the large uncertainties in A_4 and in A_2 favour the second-order fit. Application of F-statistics indicates the same conclusion. The results are independent whether the point at $\cos(\theta) = -1$ is excluded or not. The negative sign of A_4 is in agreement with a theoretical prediction [14] as well as with phase-shift analyses [1, 5]. On the other hand, corresponding fits to data in this

energy range [4] yield positive values. From phase⁴ shift analysis it is known that all terms in d-waves are small. Only $\Re(a_6)$ is of some size. If we neglect all other terms one gets

$$A_4 = \frac{1}{28} \left\{ |a_6|^2 + \Re \left[18(a_3 a_6^*) + 10\sqrt{5}(a_4 a_6^*) \right] \right\}. \quad (6)$$

The first term is positive and the second negative. This yields a cancelation making the resulting value even smaller in agreement with the present result. For the sake of simplicity we rely on the second order fit. This choice may introduce a systematical error. However, the change in the quantity of interest, i. e. the ratio A_2/A_0 is small; both results agree with each other within error bars. The second order fit is also shown in Fig. 3 as solid curve. Since A_0 is the total cross

TABLE I: Fitted Legendre polynomial coefficients (Eq. 1) in μb

parameter	second order	fourth order
A_0	230.1 ± 1.2	228.5 ± 1.5
A_2	197.0 ± 3.1	190.8 ± 5.1
A_4		-6.02 ± 3.9

section we have from the second order fit a value $\sigma = 230.1 \pm 3.6$ (*stat*) ± 23.0 (*sys*) μb with the systematical uncertainty discussed above. The efficiency correction is angle dependent, varying from 17% to 22% in the presently measured range. If a 10% precision of this correction is assumed, it adds 1.5% to the uncertainty in the total cross section only. This uncertainty is added in quadrature to the fit error and is contained in the statistical uncertainty. We compare the present angular distribution with a prediction from the SAID phase shift analysis [5], shown as dotted curve in Fig. 3. The prediction is always $\approx 10\%$ below the data. This is just the sum of all systematic errors of the present experiment. Whether this is the reason for the disagreement or not will be discussed below. From the result in the Table an anisotropy $A_2/A_0 = 0.856 \pm 0.014$ (*fit*) ± 0.0045 (*effic. corr.*) is obtained. This is close to the SAID prediction of 0.89 indicating the good reproduction of the shape of differential cross sections.

This ratio is compared in Fig. 4 with previous results [15, 16, 17]. The point joins the data in the upper part of the band formed by the experiments and is in agreement with the extrapolation of the low energy results assuming a dependence $A_2 \propto \eta^3$. However, it is 15% larger than the Pasyuk et al. result. This seems to be a large discrepancy since only the shape of the angular distributions are compared. Also shown in Fig. 4 is the prediction from fit E in Ref. [18] under the assumption of no interference at all: $A_2/A_0 = \alpha_1 \eta^3 / (\alpha_0 \eta + \alpha_1 \eta^3)$ (compare Eq. 5).

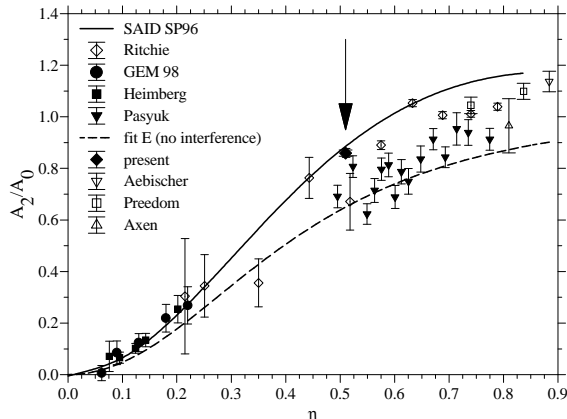


FIG. 4: Deduced ratio A_2/A_0 as function of the dimensionless pion momentum. The presently deduced value is indicated by the arrow. The earlier data are indicated by different symbols. The SAID calculation is shown as solid curve, the calculation with the assumption of no interference as dashed curve.

It should be mentioned that the quality of fits for the total cross sections for the phase shift analysis and fit E from Ref. [18] is similar, except for the near threshold region. However, the corresponding data are in the fit E but not in the SAID analysis. We have also inspected the results of the phase shift analysis solution C500. It only differs very slightly in the range $\eta < 0.35$ from the solution SP96 and gives almost identical results for larger η -values. It is worth mentioning that in Eq. 3, according to SAID, the term $\Re(a_0 a_2^*)$ is several orders of magnitude larger than all the others, except the $|a_2|^2$ term.

IV. DISCUSSION

An almost complete angular distribution for the reaction $pp \rightarrow d\pi^+$ at a beam momentum of 850 MeV/c was measured. This corresponds to a pion centre of mass momentum $\eta = p_\pi/m_\pi = 0.51$. The measurement was performed with a solid state detector with axial symmetry for larger angles and a magnetic spectrograph for emission angles close to the primary beam. The angular distribution shows a large anisotropy when compared to data closer to the threshold. This is an indication that p-wave emission is the dominant reaction mechanism. Because d-wave amplitudes are much smaller than

the s- and p-wave amplitudes one cannot extract their strength from the total cross section. The angular distribution is more sensitive to these waves. The present data give almost no evidence for a d-wave contribution to the angular distribution. Precise measurements at somewhat higher energies are desirable to investigate the importance of d-waves esp. the sign of the Legendre coefficient A_4 in the range below the resonance. The ratio A_2/A_0 does not demand d-waves. However, they contribute to the scattering asymmetry via interferences with p-waves having larger amplitudes. The weakness of d-wave amplitudes was also recently found in the measurement of spin transfer coefficients even at 400 MeV beam energy [19].

The present measurement confirms a larger ratio A_2/A_0 as extracted from recent measurements at lower beam momenta and is in good agreement with the phase shift analysis of the Virginia group. It disagrees with the results of Ref. [8]. However, these data show a large scatter which is surprising, since the comparison is made on a relative base. It has its origin mainly in large fluctuations of the A_2 values. The agreement between the new data and the SP96 solution, which does not include these data, is much better than the earlier phase shift analysis [1]. The present total cross section $\sigma = A_0$ and the second Legendre coefficient A_2 are larger than the SP96 solution but the ratio A_2/A_0 is in excellent agreement with this solution. A non negligible value for a_0 , as is applied in the SP96 solution, is confirmed by the present measurement. One needs more observables than the presently measured ones to deduce the amplitudes. Since the present result is in agreement with the SP96 solution we will rely on this solution. It yields for the ratio $|a_0|/|a_2|$ a value of 0.099 close to threshold and 0.096 for the present beam momentum. This can be compared to the result obtained by Ref. [7]. From cross section and polarisation measurements, which, together with the above cited Watson theorem, a ratio $|a_0|/|a_2| = (9 \pm 36) * 10^{-3}$ was extracted, a value which is compatible with zero.

V. ACKNOWLEDGEMENT

We are grateful to the COSY operation crew for their efforts making a good beam. Support by BMBF Germany (06 MS 568 I TP4), Internationales Büro des BMBF (X081.24 and 211.6), SCSR Poland (2P302 025 and 2P03B 88 08), and COSY Jülich is gratefully acknowledged.

-
- [1] D. V. Bugg, J. Phys. G 10, 47(1984), D. V. Bugg, A. Hasan, R. L. Shypit, Nucl. Phys. A 477, 546 (1988).
 - [2] K. Watson, Phys. Rev. 95, 228 (1954).
 - [3] P. Heimberg, priv. communication to H. M. (1999).
 - [4] B. G. Ritchie et al., Phys. Rev. C 24, 552 (1981); Phys. Rev. Lett. 66, 568 (1991); Phys. Rev. C 47, 21 (1993).
 - [5] C. H. Oh et al., Phys. Rev. C 56, 635 (1997).
 - [6] M. Drochner et al., Phys. Rev. Lett. 77, 454 (1996); Nucl. Phys. A643, 55 (1998).
 - [7] P. Heimberg et al., Phys. Rev. Lett. 77, 1012 (1996).
 - [8] E. A. Pasyuk et al., Phys. Rev. C 55, 1026 (1997).
 - [9] F. Mandl and T. T. Regge, Phys. Rev. 99, 1478 (1955).
 - [10] V. Jaeckle, K. Kilian, H. Machner, Ch. Nake, W. Oelert, P. Turek, Nucl. Instruments and Methods in Physics Research A 349, 15 (1994).
 - [11] M. Betigeri et al., Nuclear Instr. Methods in Physics Research A 421, 447 (1999).
 - [12] W. Garske, Ph. D. Thesis, Universität Münster (1999).
 - [13] H. Machner et al., Nucl. Instr. Methods for Physics Research A 437, 419 (1999).
 - [14] J. A. Niskanen, Nucl. Phys. A 298, 417 (1978).
 - [15] D. Aebischer et al., Nucl. Phys. B 108, 214 (1976).
 - [16] D. Axen et al., Nucl. Phys. A 256, 387 (1976).
 - [17] B. M. Predom et al., Phys. Lett. 65B, 31 (1976).
 - [18] H. Machner, Nucl. Phys. A 633, 341 (1998).
 - [19] B. v. Przewoski et al, Phys. Rev. C61, 064604 (2000).